Chinese J. of Chem. Eng., **9** (4) 348 – 353 (2001)

A Potential Model for Cylindrical Pores*

ZHANG Xianren(张现仁) and WANG Wenchuan(汪文川)**
College of Chemical Engineering, Beijing University of Chemical Technology, Beijing 100029, China

Abstract An analytical potential for cylindrical pores has been derived by introducing a variational method into the integration for the calculation of the interaction energy between the wall molecules and a test molecule, all of which are represented by Lennard-Jones potential. The model proposed gives good fit to the results from the cylindrical surface model and the pseudoatom model. To test the potential proposed rigorously, we have carried out grand canonical ensemble Monte Carlo(GCMC) simulation of nitrogen in the MCM-41 pore at 77 K, and compared the simulated adsorption isotherm with the experimental data reported in the literature. The simulated isotherm from our model is in almost qualitative agreement with experiment. Consequently, the model proposed provides an explicit and accurate description of cylindrical pores represented by the Lennard-Jones potential. Moreover, the model can be easily applied to a variety of cylindrical pores, ranging from cylindrical surface to finite thickness walls, in both theoretical studies and computer simulations.
Keywords potential model, cylindrical pores, GCMC, MCM-41

1 INTRODUCTION

Microporous and mesoporous materials, such as zeolites, aluminosilicates, activated carbon, and pillared clays, have a wide range of industrial applications, including heterogeneous catalysis, purification of gases and water streams, and storage of gaseous fuels. Computer simulation plays an important role in studying equilibrium and transport properties of confined fluids, and many studies have been reported with Monte Carlo (MC) or molecular dynamic (MD) methods. In most cases, slit pores are used to describe the graphite surface or activate carbon. The interaction between the slit walls and molecules in pores are represent by the Steele's 10-4-3 potential model[1,2], and the potential has been used extensively[3−10]. The discovery of novel materials with cylindrical pores, such as MCM-41[11,12] and Buckytube[13−15] has drawn much attention in recent years. However, the lack of a simple, analytical potential model for the description of the interaction between cylindrical wall and molecules in the pore incurs some inconveniences and difficulties in theoretical studies and computer simulations[16−22].

At present, there are four potential models available for cylindrical pores. (1) A potential function proposed by Tjatjopoulos *et al.*[23]. This model is derived for cylindrical surface. Therefore, it is inconvenient to use it for a pore with finite wall thickness. Besides, the hypergeometric function with infinite terms is needed in the potential expression. (2) The potential model as the analog of 10-4-3 for planar graphite surface[16]. However, this simple analog has not been refined. (3) The pseudoatom model proposed by Nicholson and Gubbins[24]. In this model, a cylindrical pore is assembled from close-packed atoms. The pore-fluid potential is calculated by the summation of pairwise atom-atom interactions between all atoms within the wall and a fluid atom. This model reflects the nature of the adsorbent, but it costs great computer time, and is unable to be used for theoretical study, for example in the density functional method. (4) The model proposed by Peterson *et al.*[25] and used by Gelb *et al.*[26]. In this model the pore-fluid potential is given by an expression, in which there are integral terms. Unfortunately, the terms can only be solved numerically[25], and this model has not been widely used yet.

This work aims at proposing a simple, analytical potential model for a cylindrical pore, in which the interactions between wall molecules and the test molecule in the pore are represented by the Lennard-Jones potential. This paper is organized as follows. First, we derive the potential model by using a variational approximation method to solve the integration for the expression of the interaction between the cylindrical wall with infinite or finite thickness and a molecule in the pore. Then, we compare our model with the model of Tjatjopoulos *et al.* for cylindrical surface, and the pseudoatom model for the cylindrical pore with finite wall thickness. Finally, to verify the model proposed, we use it for grand canonical ensemble Monte Carlo (GCMC) simulation of the adsorption of nitrogen in the adsorbent MCM-41, and compare our results with experimental data in the literature.

Received 2000-09-13, accepted 2001-04-03.
* Supported by the National Natural Science Foundation of China (No. 29776004) and the National High Performance Computing Center of China for providing the Dawning 1000A computer (No. 99118).
** To whom correspondence should be addressed.

2 INTERACTION POTENTIAL

2.1 Potential model

The potential energy of interaction between a test fluid molecule and a single molecule (or an atom) within the wall is assumed to be given by the Lennard-Jones (LJ) expression

$$u(r) = 4\varepsilon\left[\left(\frac{\sigma}{r'}\right)^{12} - \left(\frac{\sigma}{r'}\right)^{6}\right] \tag{1}$$

where r' is the intermolecular separation, σ is the collision diameter, and ε is the depth of the potential well. Assuming that the atoms of the wall are distributed continuously and uniformly within the whole region of the wall, we obtain the interaction energy, U, of the test molecule with a unit volume of the wall, V, having the number density n of the wall molecules, in cylindrical coordinates

$$U = n\int_V u(r)\mathrm{d}V = 4n\varepsilon\int_V \mathrm{d}V\left[\left(\frac{\sigma}{r'}\right)^{12} - \left(\frac{\sigma}{r'}\right)^{6}\right] \tag{2}$$

where $r'^2 = r^2 + z^2$ and z is the projection of r' along Z axis. The definition of the coordinate system and notation used for integration are shown in Fig. 1.

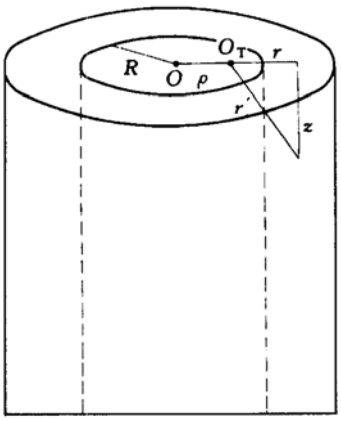

Figure 1 Definition of the coordinate system and notation used for integration

Transforming all the variables into dimensionless form, we get

$$\begin{aligned} U^* =& n^*\int_V u(r^*)\mathrm{d}V^* \\ =& 4n^*\iiint_{V^*}\left(\frac{1}{r'^{*12}} - \frac{1}{r'^{*6}}\right) r^*\mathrm{d}r^*\mathrm{d}\varphi\mathrm{d}z^* \end{aligned} \tag{3}$$

where $U^* = U/\varepsilon$, $r'^* = r'/\sigma$, $r^* = r/\sigma$, $n^* = n\sigma^3$, $\mathrm{d}V^* = \mathrm{d}V/\sigma^3$, and $r'^{*2} = r^{*2} + z^{*2}$.

To simplify our description, we omit the superscript asterisk $(*)$ of the reduced variables in the derivation hereafter, and unless pointed out, all the variables are in reduced unit. Using notation of Fig. 1 and first integrating Eq. (3) over z from 0 to $+\infty$, we get

$$\begin{aligned} U =& \frac{63\pi n}{64}\iint_S \frac{1}{r^{11}} r\mathrm{d}r\mathrm{d}\varphi - \frac{3\pi n}{2}\iint_S \frac{1}{r^5} r\mathrm{d}r\mathrm{d}\varphi \\ =& \frac{63\pi n}{64} I_1 - \frac{3\pi n}{2} I_2 \end{aligned} \tag{4}$$

where

$$I_1 = \iint_S \frac{1}{r^{11}} r\mathrm{d}r\mathrm{d}\varphi \tag{5}$$

and

$$I_2 = \iint_S \frac{1}{r^5} r\mathrm{d}r\mathrm{d}\varphi \tag{6}$$

In Eqs. (5) and (6), S represents the cross sectional area for integration, shown in Fig. 2. The next integration is over r and φ. We divide the above integrations into two regions. As is shown in Fig. 2, the first region is an accentric ring, while the second region is a homogeneous area up to infinite, represented by "I" and "II", respectively. For the two regions, I_1 and I_2 are expressed as

$$\begin{aligned} I_1 =& \int_{R-\rho}^{R+\rho} \frac{\varphi_0}{r^{10}}\mathrm{d}r + \int_{R+\rho}^{\infty} 2\pi\frac{\mathrm{d}r}{r^{10}} \\ =& 2\int_{R-\rho}^{R+\rho} \arccos\left(\frac{R^2 - \rho^2 - r^2}{2\rho r}\right)\frac{1}{r^{10}}\mathrm{d}r + \\ & \int_{R+\rho}^{\infty} 2\pi\frac{\mathrm{d}r}{r^{10}} \end{aligned} \tag{7}$$

$$\begin{aligned} I_2 =& \int_{R-\rho}^{R+\rho} \frac{\varphi_0}{r^5}\mathrm{d}r + \int_{R+\rho}^{\infty} 2\pi\frac{dr}{r^5} \\ =& 2\int_{R-\rho}^{R+\rho} \arccos\left(\frac{R^2 - \rho^2 - r^2}{2\rho r}\right)\frac{1}{r^5}\mathrm{d}r + \\ & \int_{R+\rho}^{\infty} 2\pi\frac{\mathrm{d}r}{r^5} \end{aligned} \tag{8}$$

where $\varphi_0 = 2\arccos\left(\dfrac{R^2 - \rho^2 - r^2}{2\rho r}\right)$.

Avoiding difficulties in analytically solving integration of the above expressions, as an approximation, we substitute $\arccos x$ with a polynomial, $a + bx + cx^2$. The variational method is used to determinate the parameters a, b and c, and $a = \pi/2$, $b = -3\pi/8$, $c = 0$. Therefore, we get

$$\arccos\left(\frac{R^2 - \rho^2 - r^2}{2\rho r}\right) \approx a + b\left(\frac{R^2 - \rho^2 - r^2}{2\rho r}\right) \tag{9}$$

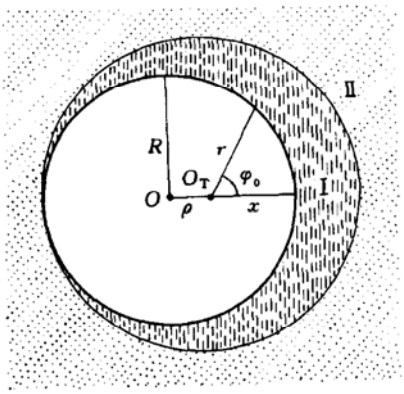

Figure 2 The region of integral

As illustration, a comparison between $\arccos x$ and $a + bx + cx^2$ is given in Fig. 3. It shows that the approximation is, in general, of good accuracy, except that discrepancies appear in the vicinity of two limits, $x = -1$ and $x = 1$. Substituting Eq. (9) into Eqs. (7) and (8), we obtain

$$U(R,\rho) = \frac{63\pi n}{64} I_1 - \frac{3\pi n}{2} I_2 \tag{10}$$

where

$$I_1 = f_1(R-\rho) - f_1(R+\rho) + \frac{2\pi}{9}\frac{1}{(R+\rho)^9} \tag{11}$$

$$I_2 = f_2(R-\rho) - f_2(R+\rho) + \frac{2\pi}{3}\frac{1}{(R+\rho)^3} \tag{12}$$

In Eqs. (11) and (12), functions f_1 and f_2 are formulated as

$$f_1(x) = \frac{\pi}{9x^9} - \frac{3\pi(R^2-\rho^2)}{80\rho x^{10}} + \frac{3\pi}{64\rho x^8} \tag{13}$$

$$f_2(x) = \frac{\pi}{3x^3} - \frac{3\pi(R^2-\rho^2)}{32\rho x^4} + \frac{3\pi}{16\rho x^2} \tag{14}$$

If the wall thickness is finite, the interaction energy of the test molecule encountered can be calculated by $U(R_1,\rho) - U(R_2,\rho)$, where R_1 and R_2 are the inside radius and outside radius of the cylindrical pore, respectively.

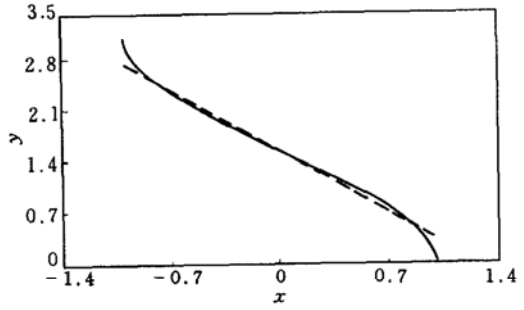

Figure 3 Comparison of arccos$x$ with $a + bx + cx^2$
—— $\arccos x$; - - - - $a + bx + cx^2$

2.2 Comparison with other potential models

We test the model proposed against two existing models: the cylindrical surface model[23] and the pseudoatom model[24]. Parameters ε_{ss} and σ_{ss}, representing the cylindrical pore, are from the simulation of molecular sieve MCM-41 by Maddox *et al.*[19]. All of the parameters in the comparisons are given in Table 1, where ε_{ff} and σ_{ff} are the parameters for the fluid in the pore, and ε_{sf} and σ_{sf} (Note: $\sigma_{sf} = \frac{\sigma_{ss}+\sigma_{ff}}{2}$) are the interaction energy and the collision diameter between solid and fluid molecules, respectively. Meanwhile, the skeletal density is 27 T-sites·nm^{-3} for the solid alone[19].

We first compare it with Tjatjopoulos' model[23] for cylindrical surface. By letting wall thickness $(R_2 - R_1)$, as small as possible, *e.g.* $(R_2 - R_1)$ being 0.00001 here, the model proposed reduces to a model for cylindrical surface, and its comparison with the model of Tjatjopoulos[23] is shown in Fig. 4.

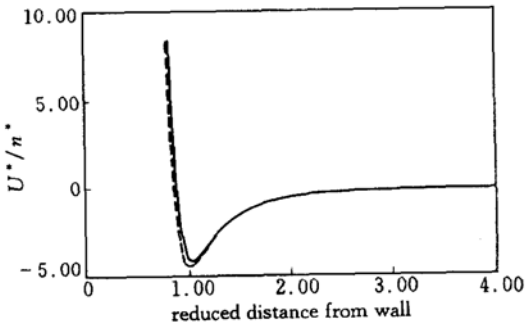

Figure 4 Comparison of the potential of cylindrical surface of Tjatjopoulos and the potential proposed, when $R_2^* - R_1^* = 0.00001$ and $R_1^* = 4$
—— this potential; - - - - Tjatjopoulos' potential

Table 1 LJ parameters representing fluid molecules and molecules within the wall of MCM-41

Case	σ_{ss}, nm	σ_{ff}, nm	σ_{sf}, nm	ε_{ss}/k, K	ε_{ff}/k, K	ε_{sf}/k, K
in comparisons of cylindrical surface model[23] and pseudoatom model[24] with this work	0.265	0.375	0.32	329	95.2	177
in GCMC simulation of adsorption of nitrogen in MCM-41, this work	0.265	0.375	0.32	236.3	95.2	150

In the pseudoatom model[24], a cylindrical pore is assembled from close-packed atoms, each of which is characterized by the LJ parameters σ_{ss} and ε_{ss}. The adsorbate potential is calculated by a summation of pairwise atom-atom interactions with a probe atom. In order to save computing time, Nicholson and Gubbins[24] calculated the potential at about 1000 locations along the cylinder radius and the data were stored for interpolation in the simulation program. Because the LJ potential is short-ranged, we here directly sum up interactions between the test molecule and all atoms inside the wall within the distance less than $5\sigma_{sf}$ to obtain the pseudoatom potential, and compare it with our potential. Fig. 5 shows the comparison of the two potentials for the cylindrical pore with the diameter of 4 nm, and the wall thickness of 2 nm.

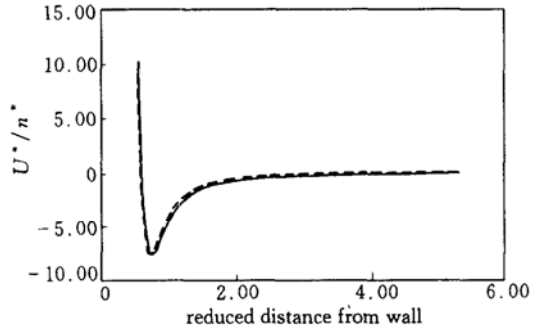

Figure 5 Comparison of interaction energy of a test atom in a cylindrical pores using pseudoatom model[24] and the model proposed (The inside diameter of the cylinder is 4 nm and the wall thickness is 2 nm)
—— this potential; - - - - pseudoatomic potential

3 GCMC SIMULATION OF ADSORPTION

It is a critical test to use the potential proposed for GCMC simulation of adsorption isotherms. Therefore, we simulate the adsorption isotherm for nitrogen in the MCM-41 pore at 77 K and compare it with experimental data.

3.1 Model

The interactions between nitrogen molecules, U_{ff}, are described by the cut and shifted LJ potential

$$U_{ff} = \begin{cases} U_{LJ}(r) - U_{LJ}(r_c) & r < r_c \\ 0 & r \geqslant r_c \end{cases} \qquad (15)$$

where r is the intermolecular distance, $r_c = 3\sigma_{ff}$, U_{LJ} is the full LJ potential given by

$$U(r) = 4\varepsilon_{ff}\left[\left(\frac{\sigma_{ff}}{r}\right)^{12} - \left(\frac{\sigma_{ff}}{r}\right)^{6}\right] \qquad (16)$$

The LJ parameters for nitrogen are taken from the literature[19], shown in Table 1. The parameters for the MCM-41 molecules, ε_{ss}, and the interaction energy parameter between a fluid molecule and the wall molecule, ε_{sf}, are also listed in Table 1. It is noticed that, similar to the work of Maddox *et al.*[19] and Nicholson and Gubbins[24], The parameters are subject to adjustments to get good agreement with experimental data. As a result, new parameters for ε_{ss} and ε_{sf} in our GCMC simulation are used (see Table 1).

3.2 GCMC simulation

In the GCMC simulation, the chemical potential of the gas phase was specified in advance. At equilibrium, the chemical potential was related to the bulk pressure in terms of an equation of state for spherical LJ model[27]. The relationship between the chemical potential and bulk pressure for LJ molecules can be referred to our previous work[28]. The initial configuration was obtained by a random placement of a few molecules in the cylindrical cell. Three types of moves were carried out with equal chances to generate a Markov chain: moving a molecule, creating a molecule, and deleting a molecule. A detailed description of the GCMC method can be obtained elsewhere[16-20,28]. The isotherms of nitrogen adsorption simulated and experimental data at 77 K by Maddox *et al.*[19] are shown in Fig. 6. For a detailed comparison with their experimental results, it is necessary to convert the number of nitrogen molecules adsorbed in a fixed length of MCM-41 into mmol·g^{-1}. We calculated the conversion factor from the experimental adsorption data in terms of the approach used by Maddox *et al.*[19].

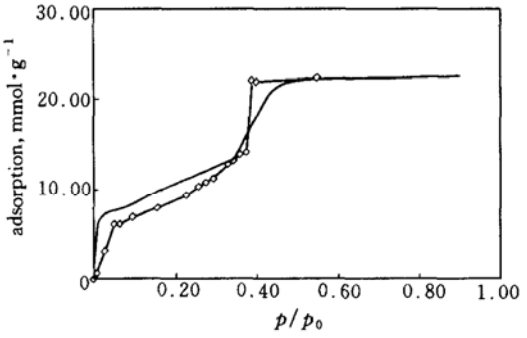

Figure 6 Adsorption isotherms for nitrogen at 77 K in MCM-41 with our model and experimental data by Maddox *et al.*[19] (pore diameter: 4 nm; thickness: 2 nm)
—□— this work; ——experimental results

4 DISCUSSION AND CONCLUSIONS

A simple analytical potential for cylindrical pores has been derived by introducing a variational method into the integration for the calculation of the interaction energy between the wall molecules and a test molecule, all of which are represented by LJ poten-

tial. In the derivation, we use an approximation, $a + bx + cx^2$, to replace $\arccos x$ in Eqs. (7) and (8) to enable the integration solved analytically. The optimum values for a, b and c are obtained in terms of the variational method. Fig. 3 gives a comparison between the two functions mentioned above. It is found that the approximation is, in general, of good accuracy, except that discrepancies appear in the vicinity of two limits, $x = -1$ and $x = 1$. However, because the integration spans a range from $x = -1$ and $x = 1$, the error in the integration can be, to some extent, canceled, as seen in Fig. 3. Consequently, Eqs. (10—14) form an explicit, simple potential model for cylindrical pores represented by LJ potential. Moreover, the model can be easily applied to diversified pores, ranging from cylindrical surface to finite thickness walls in both theoretical studies and computer simulations.

We have tested the potential proposed by comparing it with two existing models. Letting the wall of a cylindrical pore as thin as possible, the potential proposed reduces to the cylindrical surface model proposed by Tjatjopoulos *et al.*[23]. As shown in Fig. 4, our model gives an excellent fit to the model of Tjatjopoulos *et al.*[23], when $r^* > 1.2$, in particular. But, it exhibits a slightly softer core and deeper well depth, which is attributed in part to that the thickness of the wall is 0.00001 in our model. Besides, the hypergeometric function with infinite terms is used in the potential expression of Tjatjopoulos *et al.*[23].

The pseudoatom model is expressed by a summation of pairwise atom-atom interactions with a test atom. It is an accurate description of cylindrical pores in nature, although it consumes great computing time. A comparison between the pseudoatom model by Nicholson and Gubbins[24] and our model is given in Fig. 5. Both models coincide very well in a wide range of the reduced distance r^* for the homogeneous MCM-41 parameters suggested by Maddox *et al.*[19].

To test the potential proposed rigorously, we have carried out GCMC simulation of nitrogen in the MCM-41 pore at 77 K, and compared the simulated adsorption isotherm with the experimental data reported in the literature[19], shown in Fig. 5. In Table 1, it is found that the interaction energy parameters in the GCMC simulation for the wall molecules, ε_{ss}, and wall-fluid molecules, ε_{sf}, are subject to adjustments for better fit to the experimental data. Because the simulated isotherm is from a highly idealized MCM-41, having the pore diameter of 4 nm, and the wall thickness of 2 nm, it shows a typical IUPAC IV type performance with capillary condensation. In our GCMC simulation, the parameters for the interactions between oxygen atoms and that between oxygen atom and nitrogen molecule are chosen reasonably as $\varepsilon_{ss}/k = 150\,\mathrm{K}$ and $\varepsilon_{sf}/k = 236.3\,\mathrm{K}$ within the range suggested by Maddox *et al.*[19]. Obviously, the simulated isotherm from our model gives almost qualitative fit to experiment. Note that the real MCM-41 used in the experiment is an adsorbent with rather complicated structure. In the simulation, we simply used homogeneous model for the MCM-41 alone. In this case, the result seems to be satisfactory. Further improvement lies in taking account into the heterogenerity of the MCM-41[19].

NOMENCLATURE

k	Boltzmann constant, $\mathrm{J\cdot K^{-1}}$
n	number density of the wall molecules
O	center of the cylindrical pore
O_T	position of test molecule
p	pressure, MPa
p_0	staturated pressure, MPa
R	radius of the pore
R_1	inside radius of the pore
R_2	outside radius of the pore
r	the projection of r' on the cross section
r'	distance from a molecule within the wall of the pore to the test molecule
U	interaction energy of the test molecule with a unit volume of the wall
$u(r)$	potential energy between two molecules
V	volume
z	the projection of r' along Z axis
ε	depth of the potential well
ρ	distance from the center of the pore to the test molecule
σ	collision diameter
φ_0	angle or radian

Superscripts

*	reduced values

Subscripts

f	adsorbed fluid
LJ	Lennard-Jones potential model
s	wall of adsorbent

REFERENCES

1 Steele, W. A., The Interaction of Gases with Solid Surface, Pergamon, Oxford (1974).

2 Steele, W. A., "The interaction of rare gas atoms with graphitized carbon black", *J. Phys. Chem.*, **83**, 817 (1978).

3 Sokolowski, S., "Adsorption of oxygen in slit-like pores: Grand canonical ensemble Monte Carlo studies", *Mol. Phys.*, **75**, 999 (1992).

4 Jiang. S., Gubbins, K. E., Zollweg, J. A., "Adsorption, isosteric heat and commensurate-incommensurate transition of methane on graphite", *Mol. Phys.*, **80**, 103 (1993).

5 Jiang, S., Gubbins, K. E., Balbuena, P. B., "Theory of adsorption of trace components", *J. Phys. Chem.*, **98**, 2403 (1994).

6 Tan, Z., Gubbins, K. E., "Selective adsorption of simple mixtures in slit pores: A model of methane-ethane mixtures in carbon", *J. Phys. Chem.*, **96**, 845 (1992).

7 Jiang, S., Rhykerd, C. L., Gubbins, K. E., "Layering, freezing transitions, capillary condensation and diffusion of methane in slit carbon pores", *Mol. Phys.*, **79**, 373 (1993).
8 Vishnyakov, A., Piotrovskaya, E. M., Brodskaya, E. N, "Monte Carlo computer simulation of adsorption of diatomic fluids in slitlike pores", *Langmuir*, **12**, 3643 (1996).
9 Yin, Y. F., McEnaney, B., Mays, T. J., "Dependence of GCMC simulations of nitrogen adsorption on activated carbons on input parameters", *Carbon*, **36**, 1425 (1998).
10 Cracknell, R. F., Nicholson, D., Gubbins, K. E., "Molecular dynamics study of the self-diffusion of supercritical methane in slit-shaped graphitic micropores", *J. Chem. Soc. Faraday Trans.*, **91**, 1377 (1995).
11 Beck, J. S., Vartuli, J. C., Roth, W. J., Leonowicz, M. E., Kresge, C. T., Schmitt, K. D., Chu, C. T. W., Olson, D. H., Sheppard, E. W., McCullen, S. B., Higgins, J. B., Schlenker, J. L., "A new family of mesoporous molecular sieves prepared with liquid crystal templates", *J. Am. Chem. Soc.*, **114**, 10834 (1992).
12 Kresge, C. T., Leonowicz, M. E., Roth, W. J., Vartuli, J. C., Beck, J. S., "Ordered mesoporous molecular sieves synthesized by a liquid-crystal template mechanism", *Nature*, **359**, 710 (1992).
13 Iijima, S., "Helical microtubules of graphitic carbon", *Nature*, **354**, 56 (1991).
14 Iijima, S., Icihashi, T., "Single-shelled carbon nanotubes of 1 nm diameter", *Nature*, **363**, 603 (1993).
15 Bethune, D. S., Hiang, C. H., deVries, M. S., Gormen, G., Savoy, R., Beyers, R., "Cobalt-catalyzed growth of carbon nanotubes with single-atomic-layer walls", *Nature*, **363**, 605 (1993).
16 Maddox, M. W., Gubbins, K. E., "Molecular simulation of fluid adsorption in Buckytubes and MCM-41", *Int. J. ThermPhys.*, **15**, 1115 (1994).
17 Maddox, M. W., Ulberg, D., Gubbins, K. E., "Molecular simulation of simple fluids and water in porous carbons", *Fluid Phase Equili.*, **104**, 145 (1995).
18 Maddox, M. W., Gubbins, K. E., "Molecular simulation of fluid adsorption in Buckytubes", *Langmuir*, **11**, 3988 (1995).
19 Maddox, M. W., Olivier, J. P., Gubbins, K. E., "Characterization of MCM-41 using molecular simulation: Heterogeneity effects", *Langmuir*, **13**, 1737 (1997).
20 Ayappa, K. G., "Simulations of binary mixture adsorption in carbon nanotubes: Transitions in adsorbed fluid composition", *Langmuir*, **14**, 880 (1998).
21 Darkrim, F., Levesque, D., "Monte Carlo simulations of hydrogen adsorption in single-walled nanotubes", *J. Chem. Phys.*, **109**, 4981 (1998).
22 Wang, Q., Johnson, J. K., "Molecular simulation of hydrogen adsorption in single-walled carbon nanotubes and idealized carbon slit pores", *J. Chem. Phys.*, **110**, 577 (1999).
23 Tjatjopoulos, G. J., Feke, D. L., Mann, J. A., "Molecule-micropore interaction potentials", *J. Phys. Chem.*, **92**, 4006 (1988).
24 Nicholson, D., Gubbins, K. E., "Selectivity inversion in the adsorption of methane-carbon dioxide mixtures", *J. Chem. Phys.*, **104**, 8126 (1996).
25 Peterson, B. K., Walton, J. P. R. B., Gubbins, K. E., "Fluid behavior in narrow pores", *J. Chem. Soc. Faraday Trans.* 2, **82**, 1789 (1986).
26 Gelb, L. D., Gubbins, K. E., "Liquid-liquid phase separation in cylindrical pores: Quench molecular dynamics and Monte Carlo simulations", *Phys. Rev. E*, **56**, 3185 (1997).
27 Johnson, J. K., Zollweg, J. A., Gubbins, K. E., "The Lennard-Jones equation of state revisited", *Mol. Phys.*, **78**, 591 (1993).
28 Cao, D., Gao, G., Wang, W., "Grand canonical ensemble Monte Carlo simulation of adsorption storage of methane in slit micropores", *J. Chem. Ind. Eng.* (China), **51**, 23 (2000). (in Chinese)